

# ChemComm

Chemical Communications

[rsc.li/chemcomm](http://rsc.li/chemcomm)



ISSN 1359-7345

**COMMUNICATION**

Roland Winter *et al.*  
Perturbation of liquid droplets of P-granule protein LAF-1 by  
the antimicrobial peptide LL-III




Cite this: *Chem. Commun.*, 2020, 56, 11577

Received 15th July 2020,  
Accepted 4th September 2020

DOI: 10.1039/d0cc04877a

rsc.li/chemcomm

# Perturbation of liquid droplets of P-granule protein LAF-1 by the antimicrobial peptide LL-III†

Rosario Oliva,‡ Sanjib K. Mukherjee,‡ Zamira Fetahaj, Simone Möbitz and Roland Winter \*

**In recent years, liquid–liquid phase separation (LLPS) has emerged as a key mechanism for intracellular organization. But there is rapidly growing evidence that LLPS may also be associated with a number of medical conditions, including neurodegenerative diseases, by acting as a modulator of pathological protein aggregation. Here we show how LLPS formed by the P-granule protein LAF-1 and RNA can be affected by antimicrobial peptides, such as LL-III, leading to enhanced formation of amorphous protein aggregates and the loss of droplet function as an efficient reaction center and organizational hub.**

Liquid–liquid phase separation (LLPS) has been shown to be of particular importance for the membrane-less organization and compartmentalization of the intracellular space.<sup>1,2</sup> Liquid condensates (also denoted coacervates) based on LLPS are involved in a wide range of cellular functions, along with acting as processing bodies or organizational hubs.<sup>3</sup> For example, liquid-droplet like intracellular RNA/protein (RNP) assemblies, germ granules and stress granules play a significant role in the regulation of gene expression.<sup>3,4</sup> They are generally formed by various disordered proteins which interact with each other and RNA through weak associative interactions.<sup>4–6</sup>

Intrinsically disordered proteins (IDP) have a strong bias in their primary structure, including a low complexity sequence (LCS), *i.e.* sequences that consist of only a few of the 20 possible amino acids, low overall hydrophobicity, and high net charge. Owing to their LCS they are prone to undergo phase separation.<sup>4–7</sup> A prominent example is the partially disordered RNA helicase protein LAF-1, which plays an important role in promoting P-granule formation in *C. elegans* by driving LLPS formation.<sup>7</sup> P-granules play an important function in cytoplasmic RNA regulation and storage of mRNA transcripts.<sup>4,7</sup> The disordered arginine/glycine-rich (RGG) domain of LAF-1 has been found to be the main responsible factor for its

propensity to form liquid phase droplets.<sup>7</sup> RGG-containing disordered proteins can self-interact, but they can also associate with RNAs to promote the formation of RNA-containing condensates.

A particular class of disordered proteins are also antimicrobial peptides (AMPs). They form an important part of the innate immune system of all living organisms and are considered as the first line of defense against infections caused by different pathogens. Due to their broad spectrum of activity, which includes antibacterial, antifungal, antiviral and anticancer properties, AMPs have attracted great attention.<sup>8,9</sup> Although, the AMPs' mode of action is still under debate, it is believed that the first step involves the interaction with the pathogen's membrane, inducing permanent damage of the lipid bilayer finally leading to the pathogen's death. Other AMPs, instead, are able to translocate through the membrane attacking intracellular targets, such as nucleic acids and proteins.<sup>10</sup> In this context, the peptide LL-III, extracted from the venom of the eusocial bee *Lasioglossum laticeps*, showed a remarkable activity against several bacterial strains (both *Gram*-positive and *Gram*-negative), fungi and cancer cells, coupled with a moderate cytotoxicity which renders this peptide a good candidate for pharmacological applications.<sup>11</sup> The LL-III is a positively charged (+6 at pH 7.4), unstructured peptide composed of 15 amino acids, half of which are hydrophobic residues and half are polar (with five Lys residues). Even if its mode of action is still largely unknown, it was demonstrated that LL-III is able to translocate across the membrane of some cancer cells, localizing mainly in the nucleolus and in granules that are formed through LLPS of proteins and/or nucleic acids.<sup>12</sup> Prompted by this stunning observation, we set out to investigate the effect of the LL-III peptide on the phase separation propensity of the LAF-1 protein in the absence and presence of polyU as model of a single-stranded RNA partner for droplet formation.<sup>7</sup>

Generally, LLPS tends to concentrate proteins inside liquid droplets allowing for a significant increase of activity. As a downside, enhanced jamming of proteins in liquid phase droplets can also trigger aggregation. Evidence is accumulating that aberrant condensates are associated with various diseases, such as cancer and neurodegeneration. Genetic mutations, environmental perturbations

*Physical Chemistry I - Biophysical Chemistry, Faculty of Chemistry and Chemical Biology, TU Dortmund University, Otto-Hahn Strasse 4a, D-44227 Dortmund, Germany. E-mail: roland.winter@tu-dortmund.de*

† Electronic supplementary information (ESI) available. See DOI: 10.1039/d0cc04877a

‡ These authors contributed equally to this work.



or drugs, such as AMPs, could compromise LLPS and droplet formation.<sup>4,12,13</sup>

For example, stress granule proteins have been found to have a significant influence on the development of amyotrophic lateral sclerosis (ALS) by initiating aggregation and undergoing liquid-to-solid phase transformation, *i.e.* fibril formation.<sup>14–16</sup> The underlying mechanism of the disease formation and progression is still poorly understood. The effect of an antimicrobial peptide, such as LL-III, on LLPS phenomena is still *terra incognita* and is hence in the focus of this work.

To directly visualize the formation of liquid phase droplets in the LLPS process in the absence and presence of the antimicrobial peptide LL-III, phase-contrast light and fluorescence microscopy studies were employed. It has been shown that LAF-1 can phase separate *in vitro* into roundish liquid droplets of micrometer size resembling P-granules,<sup>7</sup> which is also confirmed here (Fig. 1A). Fig. 1B–D show that droplet formation of LAF-1 is drastically affected by the antimicrobial peptide. LL-III partitions into the protein-rich droplet phase and compromises droplet formation of LAF-1 in a LL-III concentration dependent manner. With increasing the concentration of the LL-III peptide (50–500  $\mu\text{M}$ ), significant disruption of the LAF-1 droplets is observed. At high peptide concentrations, the liquid droplets even transform into solid-like amorphous aggregates (Fig. 1D).

The phase boundary of LAF-1's LLPS region strongly depends on the salt concentration,<sup>13</sup> implying that intermolecular electrostatic interactions are the main driving force for the formation of the droplet assembly. The addition of NaCl (>0.4 M) leads to the dissolution of droplets without any protein aggregation. The full-length protein contains a disordered N- and C-terminus, but is predominantly  $\alpha$ -helical. The N-terminus of LAF-1 contains an intrinsically disordered RGG domain which is responsible for driving LAF-1 phase separation into liquid-like droplets.<sup>7</sup> The LAF-1 protein, with an isoelectric point of 6.6, is positively charged at pH 7.4, as is the LL-III with its five Lys residues. Hence, the main forces driving the protein-peptide interaction and aggregation are most likely hydrophobic interactions. To better assess the forces



Fig. 2 (A) Binding isotherm recorded by means of steady-state fluorescence anisotropy. The experiment was performed by titrating a 4  $\mu\text{M}$  solution of carboxyfluorescein-labeled LL-III with LAF-1 (0–10  $\mu\text{M}$ ) in the presence of 0.5 M NaCl. At these solution conditions, LAF-1 is not phase separated (results of the model fit:  $K_b = (2.6 \pm 1.3) \times 10^6 \text{ M}^{-1}$ ,  $n = 1.2 \pm 0.2$ ). (B) Circular dichroism spectra of 10  $\mu\text{M}$  LAF-1 (black line), 300  $\mu\text{M}$  LL-III peptide (red line) and of LAF-1 + LL-III mixed at the same concentrations (blue line). All experiments were carried out in 20 mM Tris-HCl, 5 mM TCEP, pH 7.4 at 25  $^{\circ}\text{C}$ .

involved in the LL-III/LAF-1 interaction, fluorescence anisotropy data of the fluorescently labeled peptide were recorded at increasing concentrations of LAF-1 in the presence of 0.5 M NaCl (Fig. 2A), *i.e.* at conditions where LAF-1 is not able to phase separate. The data were fitted with an equivalent and independent sites binding model. The analysis revealed that, on average, one LL-III molecule interacts with one LAF-1 protein with a binding constant,  $K_b$ , of  $(2.6 \pm 1.3) \times 10^6 \text{ M}^{-1}$ , pointing to a rather strong and specific interaction. Moreover, owing to charge screening at this high salt concentration, the main driving force for the interaction seems to be of hydrophobic nature. Indeed, clusters of hydrophobic residues are present in the primary sequence of LAF-1 that could represent 'hot spots' for the interaction with the LL-III peptide. However, electrostatic interactions among patches of opposite charge cannot be excluded *a priori*. Colocalization of LL-III peptide into the LAF-1 droplets is confirmed by fluorescence microscopy using fluorescently labeled LL-III (Fig. S1, ESI†).

RNA is a further major component of P-granules next to LAF-1 and is a negatively charged polymer. RNA does not markedly change the phase transition region of LAF-1, but decreases the droplet viscosity.<sup>7</sup> LAF-1 binds RNA with high affinity and RNA-induced fluidization results from highly dynamic RNA-protein interactions.<sup>7</sup> We used a poly-uridine model RNA (polyU 20) to reveal the effect of LL-III also on the LAF-1/RNA droplet assembly (Fig. S2, ESI†). Upon inspection under the microscope we observed that the poly U20 RNA colocalizes in the droplet phase of LAF-1 (Fig. S3, ESI†) and that the deteriorating effect of LL-III on LAF-1/RNA droplet formation is independent of the presence of the RNA.

To further explore the effect of the LL-III peptide on LAF-1 droplets and their morphological transformation, fluorescence spectra of the probe ThT were recorded. ThT is a fluorescent probe which is widely used to detect amyloid fibril formation.<sup>17</sup> Upon binding to amyloid fibrils, a very strong fluorescence signal is observed, which is indicative of cross- $\beta$ -sheet formation. The strong fluorescence intensity of ThT bound to fibrils is due to the loss of internal aromatic ring rotation upon binding.<sup>17</sup> However, ThT binding is not only restricted to fibrillar cross- $\beta$ -sheets, it also binds



Fig. 1 Light microscopy snapshots of LAF-1 (5  $\mu\text{M}$ ) at 25  $^{\circ}\text{C}$  in buffer (20 mM Tris-HCl, 5 mM TCEP, pH 7.4) in the absence (A) and presence of (B) 50  $\mu\text{M}$  LL-III, (C) 200  $\mu\text{M}$  LL-III, and (D) 500  $\mu\text{M}$  LL-III. (Scale bar, 20  $\mu\text{m}$ .)





to some extent to oligomers and aggregates and hydrophobic pockets *via*  $\pi$ - $\pi$  interactions of aromatic residues, with low intensity, however.<sup>18,19</sup> Fig. S4 and S5 (ESI<sup>†</sup>) depict the fluorescence spectra of 20  $\mu$ M ThT free in solution, in the presence of 5  $\mu$ M LAF-1 and in increasing concentrations of LL-III. As a control, the ThT spectrum in the presence of 50  $\mu$ M peptide was also recorded, showing that ThT is not able to bind to LL-III.

The fluorescence spectra of ThT in buffer display a broad maximum located at  $\sim$ 485 nm. In the presence of 5  $\mu$ M LAF-1 in its droplet state, an enhancement of fluorescence intensity is observed, coupled with the appearance of the band around 468 nm. The fluorescence intensity of ThT increases  $\sim$ 2.3 times only with respect to ThT in neat buffer, clearly indicating that LAF-1 does not adopt a cross- $\beta$ -sheet structure when phase separated (Fig. S4 and S5 ESI<sup>†</sup>, see also CD spectra in Fig. 2B). The blue-shifted band appearing at 468 nm is most likely due to the interaction of ThT with some hydrophobic patches of LAF-1. With increasing LL-III peptide concentration, we observed a marked decrease in ThT fluorescence intensity; in particular, the blue-shifted band is strongly affected. At the highest peptide concentration employed here (100  $\mu$ M), the ThT spectrum resembles the one obtained for ThT in pure buffer. These results strongly support the phase-separation-breaking propensity of LL-III upon direct interaction with LAF-1, in agreement with the phase contrast microscopy data which indicate loss of droplets and formation of amorphous aggregates at high LL-III concentrations (Fig. 1). This process leads to the release of ThT from the LAF-1 droplet phase, *i.e.* the ThT is not binding to LAF-1 anymore. The absence of a strong ThT fluorescence signal in the aggregated state of LAF-1 and LL-III clearly indicates that no cross- $\beta$ -sheets structures reminiscent of solid fibril formation are formed.

To further support these findings, fluorescence spectra of the probe ANS (8-anilinonaphthalene-1-sulfonic acid) in the presence of 5  $\mu$ M LAF-1, 200  $\mu$ M LL-III and LAF-1 + LL-III at the same concentrations were recorded. The probe ANS is characterized by a low quantum yield when free in solution. Upon binding to hydrophobic patches or charged residues of proteins, a strong fluorescence enhancement and blue shift of the maximum of emission is observed.<sup>20</sup> As reported in Fig. S6 (ESI<sup>†</sup>), the free ANS shows a weak fluorescence peak centred at  $\sim$ 490 nm. In the presence of LAF-1, a blue shift (to  $\sim$ 466 nm) is observed whereas the intensity remains essentially the same, suggesting that ANS can partition inside the LAF-1 droplets, most likely interacting with some hydrophobic regions of the protein or charged residues, leading to the blue shift observed. The low fluorescence enhancement detected indicates that the motion of ANS is not severely restricted, *i.e.* ANS experiences still a highly dynamic and sufficiently hydrated environment in the droplet state of LAF-1. In the presence of 200  $\mu$ M LL-III, a blue shift and a small intensity increase is detected, consistent with a weak interaction of ANS with some hydrophobic and/or charged residues of the peptide. In the presence of both LAF-1 and LL-III, a strong fluorescence intensity increase is seen, suggesting that, now, ANS is located in the highly motionally restricted and dehydrated environment of the amorphous aggregates formed by LAF-1 and LL-III.

Circular dichroism (CD) spectroscopy was finally employed to determine secondary conformational changes in LAF-1 and LL-III upon their interaction. Fig. 2B depicts the CD spectra of 5  $\mu$ M LAF-1, 300  $\mu$ M LL-III, and of LAF-1 upon addition of LL-III. The CD spectrum of LAF-1 presents two negative bands, at  $\sim$ 208 nm and  $\sim$ 220 nm, and an increase of the signal around 190 nm. These features are indicative of an  $\alpha$ -helical structure. The absence of a clear maximum at 190 indicates the presence of some random coil structures, consistent with the known secondary structure elements of the protein.<sup>7</sup> The previously recorded CD spectra of LAF-1 were acquired at non-phase-separating (high salt) conditions,<sup>7</sup> signifying that no significant conformational changes occur upon coacervation of LAF-1. Conversely, the LL-III peptide is completely disordered in solution, as can be inferred from the typical strong negative CD band around 197 nm as observed also for other short peptides.<sup>21</sup> Fig. 2B shows that when LAF-1 and LL-III are mixed, no conformational changes of LAF-1 and/or LL-III are detected, and the CD spectrum resembles the one when adding the separate CD spectra of LAF-1 and LL-III (Fig. S7, ESI<sup>†</sup>). Of note, even if the absolute concentrations of LAF-1 and LL-III are different here, due to the different sizes of the interacting partners (LL-III 15 a.a. residues, LAF-1 708 a.a. residues), the concentrations of the chromophore, *i.e.* the number of amide bonds, are comparable. Hence, we can conclude that no significant conformational changes occur upon binding of LL-III to LAF-1 and aggregate formation.

Fig. 3 depicts a schematic representation of the effect the LL-III peptide is imposing on the phase separation propensity and droplet formation of LAF-1. Before the addition of the peptide, 5  $\mu$ M LAF-1 is phase separated, forming liquid phase droplets. Upon addition of LL-III, the peptide first partitions inside the droplets and, through hydrophobic and electrostatic interactions, strongly interacts with LAF-1 protein, leading to the formation of amorphous solid aggregates and disintegration of the biocondensate. It is important to note that the formation of the aggregates does not cause any major conformational changes of the interacting partners.

It is well known that LLPS can strongly modulate a series of cellular functions, such as enzymatic reactions and ligand binding.<sup>20–22</sup> To finally demonstrate the impact of LL-III on the functionality of the droplet condensate, the kinetics of an



Fig. 3 Schematic representation of the LAF-1 liquid droplet-breaking ability of the LL-III peptide. LL-III is shown in yellow, the LAF-1 protein in black and red (the thicker line represents the N-terminus of LAF-1, the red cylinder its  $\alpha$ -helical region, and the thinner line the C-terminus). The relative sizes of LAF-1 and LL-III are not to scale.



enzymatic reaction when partitioning into the LAF-1 condensate was studied by following the hydrolysis reaction of the fluorescent substrate Ala-Ala-Phe-7-amido-4-methylcoumarin (AAF-AMC) catalyzed by  $\alpha$ -chymotrypsin ( $\alpha$ -CT). The hydrolysis of the substrate's amide bond between the Phe residue and the coumarin (AMC) leads to the release of AMC which can be followed by fluorescence spectroscopy. We evaluated the slope of the linear portion of the fluorescence intensity vs. time plot (Fig. S8, ESI†), which is directly proportional to the initial rate constant of the reaction,  $v_0$ . Fig. S9 (ESI†) reports relative  $v_0$  values in the absence and presence of LAF-1 and upon addition of different amounts of the antimicrobial peptide LL-III. For the reaction carried out in pure buffer, a slope of  $15.7 \pm 2.1$  was recorded. In the presence of  $5 \mu\text{M}$  LAF-1, we observe a strong increase in the reaction rate (slope of  $32.3 \pm 1.4$ ), indicating that both  $\alpha$ -CT and AAF-AMC partition into the LAF-1 droplets, thereby increasing their local concentration which leads to the marked increase of the reaction rate. Such drastic acceleration of the reaction rate is a hallmark of LLPS when both reaction partners partition into the dense droplet phase. Upon addition of  $10 \mu\text{M}$  to  $200 \mu\text{M}$  of LL-III, a progressive decrease of the reaction rate is detected. At  $200 \mu\text{M}$  of LL-III, the reaction rate is comparable to the one in neat buffer. These data indicate that upon interaction of LL-III with LAF-1, which finally leads to the loss of the liquid-like droplet state and formation of amorphous solid aggregates, the enzyme and the substrate are released into the bulk solution, restoring the original reaction rate in pure buffer. Hence, the interaction of LL-III with LAF-1 leads to the loss of the droplet phase with dramatic effects on the enzymatic activity and probably on all biochemical processes taking place inside the droplets, resulting in a massive restriction of their functionality. Control experiments in the presence of neat LL-III peptide show that the peptide itself has some inhibitory effect on the hydrolysis reaction because LL-III has the potential to act as substrate as well. Thus, the decrease of the reaction rate in LAF-1 droplets is expected to be due to the inhibitory effect of LL-III in conjunction with the peptide perturbing the droplet structure by intermolecular interactions of LL-III with LAF-1, finally leading to formation of protein aggregates and the release of the enzyme and substrate to the bulk solution.

To conclude, many studies on RNA/protein assemblies in recent years have provided important insights into the role of LLPS in normal cell biology.<sup>1–4</sup> Further, there is rapidly growing evidence that LLPS may also be associated with a number of medical conditions, including neurodegenerative diseases, acting as a modulator of pathological protein aggregation.<sup>14–16</sup> Here we present, to our knowledge for the first time, how LLPS is affected by an antimicrobial peptide. We show that antimicrobial peptides such as LL-III are able to interact strongly with liquid phase droplets, leading to the loss of their function as efficient reaction centers and organizational hubs. In our case of the LAF-1, a RNA helicase, this will lead to malfunction of important intracellular RNA microreactors, the P-granules. Generally, such disturbed phase separation and impeded

condensate formation might drive aberrant transcriptional programs leading to neurodegeneration, cancer and infection diseases. On the other hand, the aggregates formed, in particular if they are of amorphous and hydrophobic character, might be toxic, similar to aggregates of amyloidogenic peptides or amyotrophic lateral sclerosis causing mutated RNA-binding proteins, such as FUS or TDP-43.<sup>4</sup> Future research on the effect of antimicrobial peptides interacting with specific liquid condensates will not only add to the understanding of complex disease mechanisms originating in poorly functioning of such condensates, but could also open up exciting new avenues for therapeutic intervention.

Financial support from the Deutsche Forschungsgemeinschaft (DFG, German Research Foundation) under Germany's Excellence Strategy – EXC 2033 – 390677874 – RESOLV is gratefully acknowledged.

## Conflicts of interest

The authors declare no conflict of interest.

## Notes and references

- 1 T. Lu and E. Spruijt, *J. Am. Chem. Soc.*, 2020, **142**, 2905–2914.
- 2 Y. Shin and C. P. Brangwynne, *Science*, 2017, **357**, eaaf4382.
- 3 S. Alberti, A. Gladfelter and T. Mittag, *Cell*, 2019, **176**, 419–434.
- 4 S. Alberti and D. Dormann, *Annu. Rev. Genet.*, 2019, **53**, 171–194.
- 5 S. F. Banani, H. O. Lee, A. A. Hyman and M. K. Rosen, *Nat. Rev. Mol. Cell Biol.*, 2017, **18**, 285–298.
- 6 C. P. Brangwynne, P. Tompa and R. V. Pappu, *Nat. Phys.*, 2015, **11**, 899–904.
- 7 S. Elbaum-Garfinkle, Y. Kim, K. Szczepaniak, C. C. Chena, C. R. Eckmann, S. Myong and C. P. Brangwynne, *Proc. Natl. Acad. Sci. U. S. A.*, 2015, **112**, 7189–7194.
- 8 K. A. Brogden, *Nat. Rev. Microbiol.*, 2005, **3**, 238–250.
- 9 B. Mishra, R. Saravanan, L. Xiang, L. K. Yang and S. S. J. Leong, *RSC Adv.*, 2013, **3**, 9534–9543.
- 10 V. Teixeira, M. J. Feio and M. Bastos, *Prog. Lipid Res.*, 2012, **51**, 149–177.
- 11 A. Vrablikova, L. Czernekova, R. Cahlikova, Z. Novy, M. Petrik, S. Imran, Z. Novak, M. Krupka, V. Cerovsky, J. Turanek and M. Raska, *Microbiol. Immunol.*, 2017, **61**, 474–481.
- 12 J. Slaninova, V. Mlsova, H. Kroupova, L. Alan, T. Tumova, L. Monincova, L. Borovickova, V. Fucik and V. Cerovsky, *Peptides*, 2012, **33**, 18–26.
- 13 C. O. Matos, Y. M. Passos, M. J. do Amaral, B. Macedo, M. H. Tempone, O. C. L. Bezerra, M. O. Moraes, M. S. Almeida, G. Weber, S. Missailidis, J. L. Silva, V. N. Uversky, A. S. Pinheiro and Y. Cordeiro, *FASEB J.*, 2020, **34**, 365–385.
- 14 A. A. Hyman, C. A. Weber and F. Julicher, *Annu. Rev. Cell Dev. Biol.*, 2014, **30**, 39–58.
- 15 Y. R. Li, O. D. King, J. Shorter and A. D. Gitler, *J. Cell Biol.*, 2013, **201**, 361–372.
- 16 T. R. Peskett, F. Rau, J. O'Driscoll, R. Patani, A. R. Lowe and H. R. Saibil, *Mol. Cell*, 2018, **70**, 588–601.
- 17 M. C. Owen, D. Gnutt, M. Gao, S. K. T. S. Wärmländer, J. Jarvet, A. Gräslund, R. Winter, S. Ebbinghaus and B. Strodel, *Chem. Soc. Rev.*, 2019, **48**, 3946–3996.
- 18 M. Groenning, *J. Chem. Biol.*, 2010, **3**, 1–18.
- 19 R. Carrotta, R. Bauer, R. Waning and C. Rischel, *Protein Sci.*, 2001, **10**, 1312–1318.
- 20 R. Oliva, S. Banerjee, H. Cinar, C. Ehrt and R. Winter, *Sci. Rep.*, 2020, **10**, 8074.
- 21 R. Oliva, P. D. Vecchio, A. Grimaldi, E. Notomista, V. Cafaro, K. Pane, V. Schuabb, R. Winter and L. Petraccone, *Phys. Chem. Chem. Phys.*, 2019, **21**, 3989–3998.
- 22 R. Oliva, S. Banerjee, H. Cinar and R. Winter, *Chem. Commun.*, 2020, **56**, 395–398.

